Mehdi Aramideh, Mahmoud Mirzaei*, Ghadamali Khodarahmi and Oğuz Gülseren

DFT Studies of Graphene-Functionalised Derivatives of Capecitabine

Abstract: Cancer is one of the major problems for so many people around the world; therefore, dedicating efforts to explore efficient therapeutic methodologies is very important for researchers of life sciences. In this case, nanostructures are expected to be carriers of medicinal compounds for targeted drug design and delivery purposes. Within this work, the graphene (Gr)-functionalised derivatives of capecitabine (CAP), as a representative anticancer, have been studied based on density functional theory calculations. Two different sizes of Gr molecular models have been used for the functionalisation of CAP counterparts, CAP-Gr3 and CAP-Gr5, to explore the effects of Gr-functionalisation on the original properties of CAP. All singular and functionalised molecular models have been optimised and the molecular and atomic scale properties have been evaluated for the optimised structures. Higher formation favourability has been obtained for CAP-Gr5 in comparison with CAP-Gr3 and better structural stability has been obtained in the water-solvated system than the isolated gas-phase system for all models. The CAP-Gr5 model could play a better role of electron transferring in comparison with the CAP-Gr3 model. As a concluding remark, the molecular properties of CAP changed from singular to functionalised models whereas the atomic properties remained almost unchanged, which is expected for a carrier not to use significant perturbations to the original properties of the carried counterpart.

Keywords: Capecitabine; Density Functional Theory; Functionalisation; Graphene.

*Corresponding author: Mahmoud Mirzaei, Department of Medicinal Chemistry, School of Pharmacy and Pharmaceutical Sciences, Isfahan University of Medical Sciences, Isfahan, Iran, E-mail: mdmirzaei@pharm.mui.ac.ir
Mehdi Aramideh and Ghadamali Khodarahmi: Department of Medicinal Chemistry, School of Pharmacy and Pharmaceutical Sciences, Isfahan University of Medical Sciences, Isfahan, Iran, E-mail: mehdiaramide@pharm.mui.ac.ir (M. Aramideh), khodarahmi@pharm.mui.ac.ir (G. Khodarahmi)
Oğuz Gülseren: Department of Physics, Faculty of Science, Bilkent University, Ankara, Turkey, E-mail: gulseren@fen.bilkent.edu.tr

1 Introduction

Cancer is one of the major problems for the health of so many people around the world, and numerous research efforts have been dedicated to explore proper solutions for this life-limiting problem [1]. Investigating more efficient therapeutic treatments for cancer are very important because of the increasing number of unwanted side effects from current treatments for patients [2–4]. One of the hopes in this case is nanoscience and technology, in which several efforts, soon after the pioneering discovery of carbon nanotubes [5], have been dedicated to investigating the applications of nanostructures in biological systems to increase the quality of living systems [6–9]. Studies have indicated that nanostructures could be considered as possible carriers for medicinal compounds in targeted drug design and delivery processes [10, 11]. To this aim, characterising the properties of nanostructures and determining their effects on the carried counterparts are very important to find the advantages of nanostructures for medicinal applications [12]. In addition to nanotubes, there are other nanostructures in which graphene (Gr), as a two-dimensional nanostructure, has stirred up the interest of so many researchers since its first discovery by Geim and Novoselov [13]. The honeycomb layer-like structures of carbon atoms, which have been known as graphite for several years, were finally characterised as single-standing monolayer Gr nanostructures [14]. Several attempts have been dedicated to investigating the various aspects and applications of this novel material, in which biology-related applications of Gr are among the most important [15–18]. Carrying medicinal compounds to specific targets in living systems is one of the supposed roles of Gr and other nanostructures to reduce the increasing number of side effects from harmful cancer therapy processes [19]. To achieve this purpose, both covalent and noncovalent functionalisations are used for Gr nanostructures to achieve functionalised models for specific therapeutic applications [20–23]. As a representative case, capecitabine (CAP) is a well-known medicinal compound for cancer therapy with high efficacy for therapy but low specificity for the target [24, 25]. Considerable efforts have been done to generate CAP derivatives with fewer side effects, among which nanostructure functionalisation is
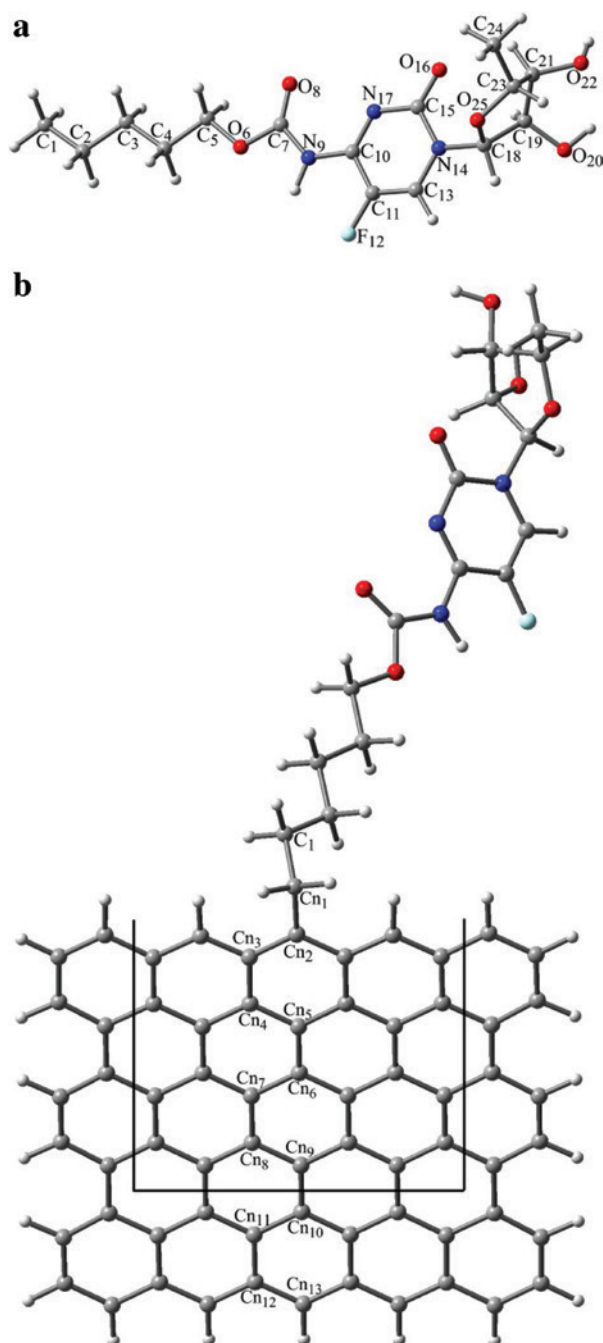
a

b

Figure 1: (a) CAP, (b) CAP-Gr3 and CAP-Gr5 (the structural region of Gr3 is shown in the box). The original Gr models are without CAP counterparts.

one of the desirable choices for the purpose [26–28]. Therefore, the careful determination of properties for functionalised systems is important to propose the applications of new hybrid structures. In this case, computational chemistry techniques could provide insightful information to investigate the different aspects of complicated biological and nano systems [29, 30].

Within this work, the possibilities and properties of Gr-functionalisation of CAP (Fig. 1) have been investigated based on quantum chemical computations. To this aim, two different sizes of Gr molecular models, Gr3 and Gr5, have been designed to be functionalised with their CAP counterparts. It is important to note that the quantum computations are mainly performed for molecular systems, in which their sizes and scales are somehow far away from the real systems. Although direct comparisons of computational and experimental works are almost impossible, the rational design of molecular systems for computational works could be possible based on experimental achievements [31]. Indeed, computational and experimental works are complementary to each other. Relating to the current work, the existence of Gr-functionalised systems in reality have been very well recognised by earlier experimental works [32–35]. Therefore, the molecular systems used in this work have been prepared based on the earlier approved concept of Gr-functionalisation. To achieve this purpose, the geometries of all singular and functionalised molecular models were optimised first and then the molecular and atomic scale properties were evaluated for the optimised structures (Tabs. 1 and 2). Different types of energies, factors of electron transfers, frontier molecular orbitals distribution patterns (Fig. 2), maximum absorption wavelengths, and nuclear magnetic resonance (NMR) properties have been evaluated to investigate the effects of Gr-functionalisation on the original properties of the CAP counterparts, as the main question of this work.

2 Computational Details

Within this work, density functional theory (DFT) calculations have been performed to investigate the stabilities and properties of the Gr-functionalised models of CAP counterparts (Fig. 1). The calculations have been done in two systems: isolated gas phase and water solvated. Two Gr molecular models have been included in the calculations based on their molecular sizes, Gr3: $C_{29}H_{16}$ and Gr5: $C_{67}H_{24}$. First, the geometries of all singular models were optimised to obtain the minimum-energy structures. Next, the obtained optimised singular structures were attached to each other to construct CAP-Gr3 and CAP-Gr5 functionalised models. Subsequently, the geometries of new functionalised models were optimised to generate stable minimised energy models. Finally, the models of this work include two sets of singular (CAP, Gr3, and Gr5) and functionalised (CAP-Gr3 and CAP-Gr5) models. The evaluated molecular properties from optimisation processes including bond distances (d) and angles ($\angle$), dipole moments

Table 1: Molecular properties: Optimised connection bond distance (d/Å), connection bond angle ($\angle$/°), total energy (E_t/eV), binding energy (E_b/eV), ionisation energy (I/eV), electron affinity (A/eV), energy gap (E_g/eV), chemical potential (μ/eV), chemical hardness (η/eV), chemical softness (σ/eV^{-1}), electrophilicity index (ω/eV), dipole moment (D_m/Debye), and maximum absorption wavelength (λ_{max}/nm).

Property[a]	CAP	Gr3	Gr5	CAP-Gr3	CAP-Gr5
d_{C1-Cn1}				1.55 [1.55]	1.55 [1.55]
$d_{Cn1-Cn2}$		1.51 [1.51]	1.51 [1.51]	1.52 [1.52]	1.52 [1.52]
$\angle_{C1-Cn1-Cn2}$				114.91 [115.12]	115.74 [115.27]
E_t	−35,381.90	−30,335.12	−69,875.97	−65,684.22	−105,225.06
	[−35,383.22][b]	[−30,336.31]	[−69,878.34]	[−65,686.65]	[−105,228.65]
E_b	4.49 [4.56]	5.60 [5.72]	6.05 [6.18]	5.08 [5.18]	5.56 [5.67]
I	6.34 [6.20]	4.33 [4.39]	3.70 [3.72]	4.41 [4.39]	3.75 [3.71]
A	1.52 [1.38]	2.51 [2.57]	3.39 [3.41]	2.59 [2.56]	3.44 [3.40]
E_g	4.82 [4.82]	1.82 [1.82]	0.31 [0.31]	1.82 [1.82]	0.31 [0.31]
μ	3.93 [3.79]	3.42 [3.48]	3.54 [3.56]	3.50 [3.48]	3.59 [3.56]
η	4.82 [4.82]	1.82 [1.82]	0.31 [0.31]	1.82 [1.82]	0.31 [0.31]
σ	0.21 [0.21]	0.55 [0.55]	3.26 [3.27]	0.55 [0.55]	3.26 [3.27]
ω	1.60 [1.49]	3.22 [3.32]	20.43 [20.76]	3.36 [3.31]	21.05 [20.67]
D_m	3.07 [4.80]	0.48 [0.94]	0.62 [0.31]	2.94 [4.26]	2.96 [2.93]
λ_{max}	224 [226]	700 [735]	636 [653]	703 [738]	637 [653]

[a]See Figure 1 for models.
[b]Water-solvated systems.

(D_m), total energies (E_t), binding energies (E_b), ionisation energy (I), electron affinity (A), energy gap (E_g), chemical potential (μ), chemical hardness (η), chemical softness (σ), and electrophilicity index (ω) have been summarised in Table 1. Furthermore, time-dependent (TD-DFT) calculations have been performed for the optimised models to evaluate maximum absorption wavelength (λ_{max}). Equations 1 to 8, as introduced by Masoodi et al. [36], have been used to evaluate the values of some of these mentioned properties.

$$E_b = ([\textstyle\sum a_i\varepsilon_i] - E_t)/\textstyle\sum a_i \tag{1}$$

$$I = -\text{HOMO} \tag{2}$$

$$A = -\text{LUMO} \tag{3}$$

$$E_g = \text{LUMO} - \text{HOMO} \tag{4}$$

$$\mu = (\text{HOMO} + \text{LUMO})/2 \tag{5}$$

$$\eta = (\text{LUMO} - \text{HOMO})/2 \tag{6}$$

$$\sigma = 1/\eta \tag{7}$$

$$\omega = \mu^2/2\eta \tag{8}$$

where a_i and e_i stand for number and energy of each atomic type of this work; H, C, N, O, F in 1. HOMO and

LUMO stand for energies of the highest occupied and the lowest unoccupied molecular orbitals in 2–6.

Moreover, isotropic chemical shifts (δ) have been evaluated for the atoms of optimised singular and functionalised models to investigate the atomic scale properties (Tab. 2, Figs. 3 and 4). First, chemical shielding tensors (s_{ii}) were calculated based on the gauge-independent atomic orbital approach [37] and then they were converted to isotropic chemical shielding (S_{iso}) using 9 [38]. Next, values of δ were generated using 10 [38], in which the calculated reference values of isotropic chemical shielding ($S_{iso,ref}$) were considered for different atomic types: $Si(CH_3)_4$ for H and C, NH_3 for N, H_2O for O, and HF for F atomic types.

$$S_{iso} = (s_{11} + s_{22} + s_{33})/3 \tag{9}$$

$$\delta = S_{iso,ref} - S_{iso,sample} \tag{10}$$

All calculations for this work were performed using the B3LYP exchange-correlation functional [39] and the 6-31G* standard basis set [40] as implemented in the Gaussian program [41] for isolated gas-phase and water-solvated systems. The polarisable continuum model [42] has been used to inlcude the water solvent in the calculations. The molecular systems in this work are all attached together through covalent bonds; therefore, the standard and much more popular theoretical level (B3LYP/6-31G*) have been used for performing calculations [43, 44]. It is worth to note that the Kohn−Sham DFT methods have

Table 2: Atomic properties: isotropic chemical shifts (δ/ppm).

Atom[a]	CAP	Gr3	Gr5	CAP-Gr3	CAP-Gr5
Cn_{13}			124 [124]		124 [124]
Cn_{12}			130 [132]		130 [132]
Cn_{11}			118 [120]		118 [120]
Cn_{10}			118 [119]		118 [120]
Cn_9		122 [123]	117 [118]	122 [123]	118 [118]
Cn_8		128 [129]	119 [120]	127 [129]	119 [120]
Cn_7		121 [122]	119 [120]	121 [122]	119 [120]
Cn_6		124 [129]	118 [118]	124 [124]	118 [119]
Cn_5		123 [129]	118 [118]	123 [123]	118 [119]
Cn_4		122 [123]	119 [120]	122 [123]	119 [120]
Cn_3		127 [128]	130 [131]	127 [128]	129 [130]
Cn_2		126 [131]	128 [136]	129 [135]	132 [140]
Cn_1		16 [16]	16 [16]	28 [28]	30 [30]
C_1	16 [16][b]			34 [34]	34 [35]
C_2	26 [27]			32 [31]	32 [32]
C_3	29 [30]			28 [28]	29 [29]
C_4	31 [31]			31 [30]	31 [31]
C_5	66 [68]			66 [67]	65 [68]
O_6	154 [164]			154 [164]	154 [164]
C_7	139 [143]			139 [141]	139 [142]
O_8	307 [293]			306 [294]	306 [294]
N_9	113 [121]			113 [121]	113 [121]
C_{10}	145 [148]			145 [147]	145 [148]
C_{11}	129 [131]			129 [130]	129 [131]
F_{12}	35 [52]			35 [52]	35 [51]
C_{13}	127 [132]			127 [131]	127 [132]
N_{14}	162 [170]			162 [169]	162 [169]
C_{15}	143 [146]			143 [145]	144 [146]
O_{16}	327 [311]			327 [311]	326 [311]
N_{17}	238 [230]			239 [230]	239 [230]
C_{18}	102 [103]			103 [102]	103 [103]
C_{19}	74 [75]			74 [74]	74 [75]
O_{20}	21 [24]			20 [25]	21 [24]
C_{21}	76 [77]			77 [76]	77 [77]
O_{22}	16 [18]			16 [18]	16 [18]
C_{23}	79 [79]			79 [78]	79 [79]
C_{24}	19 [20]			19 [19]	[20]
O_{25}	80 [83]			81 [84]	80 [84]

[a]See Figure 1 for models and atomic position numbers.
[b]Water-solvated systems.

helped researchers to investigate various characteristic properties of materials and reactions based on standard computational methodologies for several years [45].

3 Results and Discussion

Within this work, the stabilities and properties for the Gr-functionalised CAP hybrid structures (CAP-Gr; capecitabine-graphene; Fig. 1) have been investigated based on DFT-calculated properties (Tabs. 1 and 2, Figs. 3 and 4) of

the optimised singular CAP and Gr counterparts have been attached to each other to represent the functionalised models (CAP-Gr3 and CAP-Gr5). The original Gr models (Gr3 and Gr5) have an extra methyl group to provide a functionalisation site for the CAP counterpart. It should be noted that one hydrogen atom should be released from each of the CAP and Gr counterparts to make covalent bonds in the functionalisation processes. The validity of such a molecular scale model has been examined previously by some other computational works [46, 47].

Examining values of E_t (total energies) from Table 1 indicates more stabilities for the molecules in the water-solvated system than in the isolated-gas phase system. However, there are no significant changes for their characteristic bond lengths and angles in two computational phases. The obtained values of E_b (binding energies) also approve more stability for the molecules in the water-solvated system than in the isolated gas-phase system, in which higher energies are needed to break the structural bonds of the water-solvated systems. The values of I (ionisation energy) and A (electron affinity) properties have been evaluated based on Koopmans' theorem [48], as a technique based on calculations of HOMO and LUMO energies. Because only approximate values could be generated from Koopmans' theorem, several attempts have been dedicated to evaluate and validate more precise results for the I and A values of chemical structures based on this theorem [49, 50]. Comparing values of I and A for Gr3 and Gr5 models reveals more favourability with electron transferring for the Gr5 model than the Gr3 model. Parallel tendencies of electron transferring have also been seen for the CAP-Gr models. The level of A has been increased whereas the level of I has been decreased for both functionalised models in comparison with the singular CAP model. Furthermore, the obtained values of E_g indicated that molecular reactivity significantly increased in the CAP-Gr models rather than in the singular CAP model. Comparing the values of I, A, and E_g for the models in the water-solvated and isolated gas-phase systems indicates slight effects of solvent on the molecular orbital levels, which have been observed by slight changes in the obtained parameters. Figure 2 demonstrates that both HOMO and LUMO patterns are distributed over the entire surface of the planar Gr3 model whereas they are distributed only at the upper/lower edges of the planar Gr5 model. The HOMO and LUMO patterns are distributed at the ring of singular CAP but they are all transferred to the Gr counterpart in the CAP-Gr hybrid models. Distribution patterns for singular and hybrid Gr structures are similar; however, these patterns for CAP structures are completely different from singular to hybrid structures. The solvent
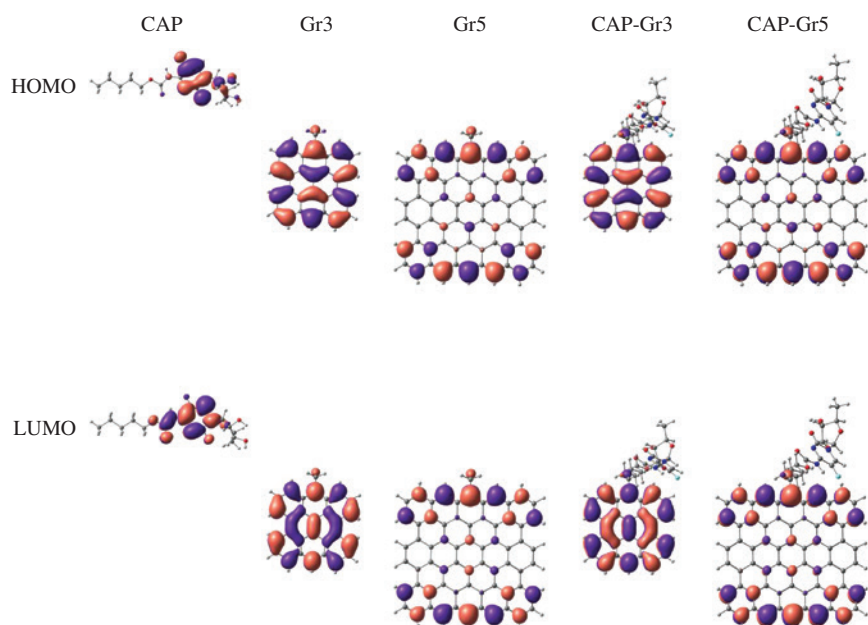
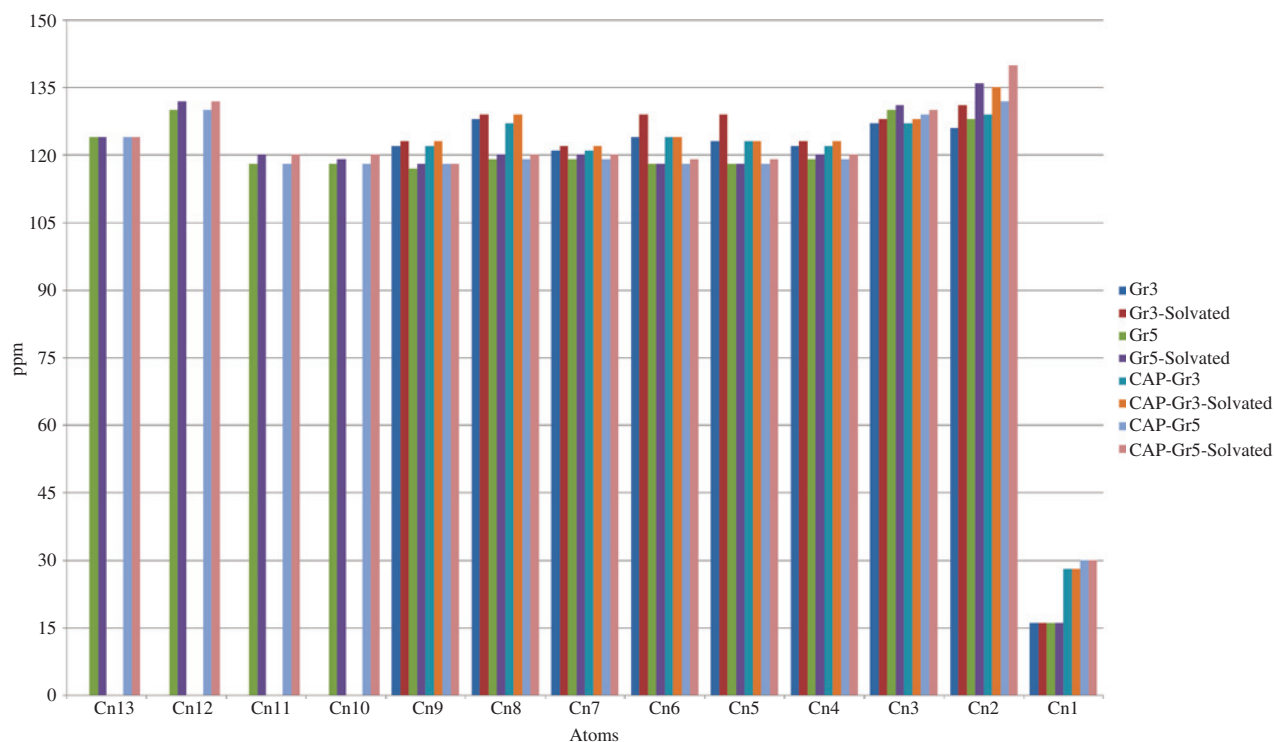**Figure 2:** HOMO and LUMO distribution patterns.

Figure 3: Graphical representations of δ values for the Gr counterparts.

effects have not been observed for the HOMO and LUMO distribution patterns. Examining the values of D_m (dipole moments) indicates that the polarities of Gr3 models are higher in water-solvated system than in the isolated gas-phase system; however, reversed results are observed for the polarities of Gr5 models in two mentioned systems. It could be somehow approved by different distribution patterns, in which the patterns are distributed on the entire surface of Gr3 models whereas they are distributed only at the upper/lower edges of Gr5 models. The obtained results
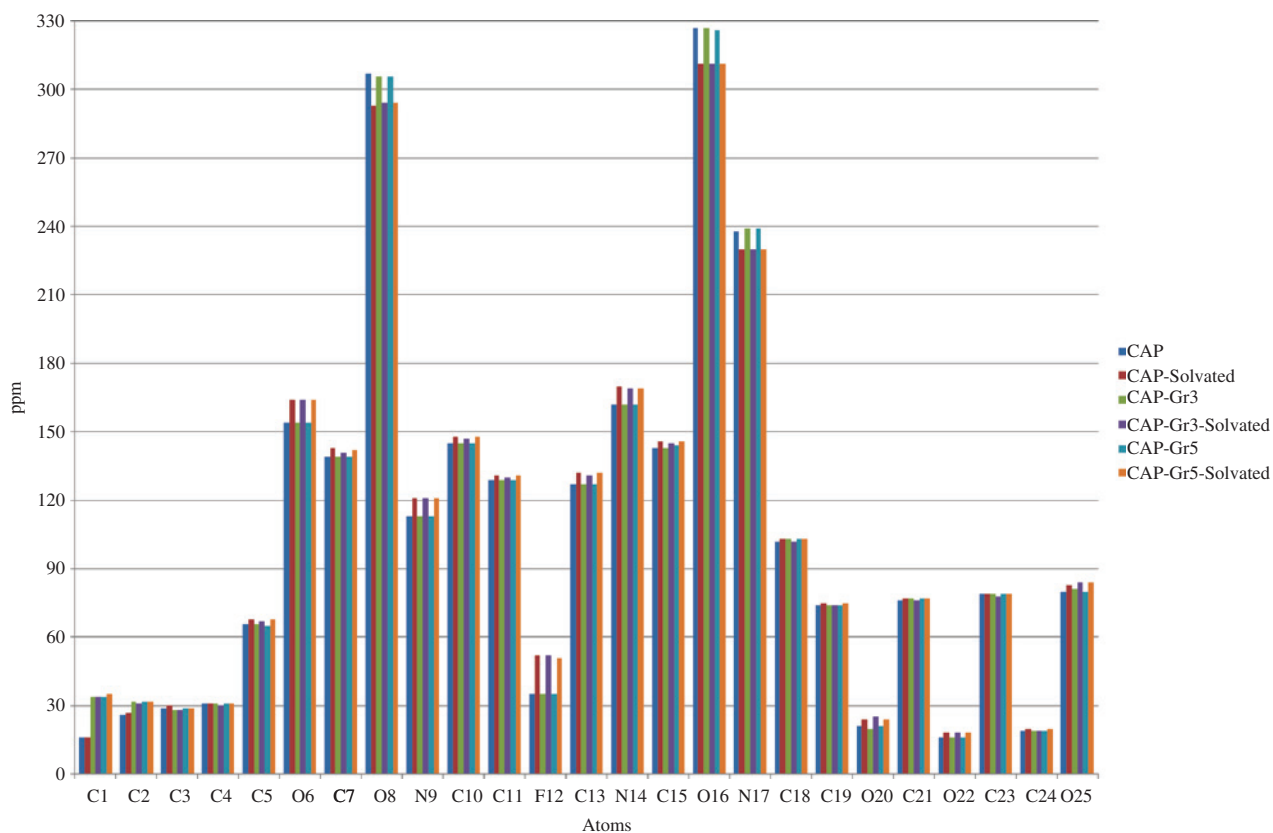
Figure 4: Graphical representations of δ values for the CAP counterparts.

of ω (electrophilicity index) indicated that the electrophilicity for Gr5 models are higher than Gr3 models, which have been earlier shown by the higher affinity of Gr5 in comparison with Gr3. The results by lower η (chemical hardness) and higher σ (chemical softness) for Gr5 models in comparison with Gr3 models also approve the trend obtained by the ω values for Gr3 and Gr5 models. In all models, the maximum absorptions of isolated gas-phase systems have been shifted to upper wavelengths in the water-solvated systems. Comparing the values of λ_{max} (maximum absorption wavelength) indicates that the absorptions will take place in longer wavelengths for Gr3 models than the Gr5 models. Because shorter wavelength stands for higher energy, the required short absorption wavelength of singular CAP would be changed into longer wavelengths for CAP-Gr models in safer regions.

Atomic-scale properties including δ (isotropic chemical shifts) have been evaluated for further investigations of the optimised models of this work based on NMR parameters (Tab. 2; Figs. 1, 3 and 4). The values of δ could demonstrate insightful information about the electronic and chemical environments of atoms in molecular systems [51, 52]. NMR is among the most versatile techniques to investigate the properties of matters in different phases

[38]. Examining the results of Table 2 and Figures 3 and 4 indicates that the δ properties could detect the effects of solvents for atomic properties of the molecular models, in which the effects are significant for N, O, and F atoms more than C atoms. The lone pairs of electrons at the N, O, and F atomic sites are important to designate the characteristic properties for their atoms regarding chemical environments. One of the important factors for using materials as carriers or containers of medicinal compounds is that the original properties of the carried counterpart should remain unchanged after hybridisation as much as possible. Careful examinations of the δ values (Fig. 4) indicate that the effects on atomic properties of CAP after hybridisation are almost negligible, with the exception of those atoms from the functionalisation region. It has been earlier indicated that the atomic dopants could change the atomic properties of the doped regions of nanostructures whereas the properties of other atoms remain almost unchanged [53, 54]. Within the current results, the atomic properties of both CAP and Gr counterparts could remain unchanged with the exceptions of those atoms in the functionalisation regions. Recalling the molecular properties, it has been demonstrated that the molecular properties of CAP-Gr models are different from the singular

CAP counterparts; however, the atomic properties could show that the original atomic-scale properties remain unchanged. As a final remark, newer molecular properties have been introduced for the molecular systems but the characteristic atomic properties show the originality of the functionalised models.

4 Conclusions

Within this work, we have investigated the CAP-Gr hybrids to explore either the effects of functionalisation on the original properties of each counterpart or the newly discovered properties for hybrid structures. To this aim, we have evaluated molecular and atomic scale properties for the considered molecular models in two isolated gas-phase and the water-solvated systems based on DFT calculations. The conclusion of this work could be summarised into some trends. First, lower total energies were obtained for the models in water-solvated systems revealing higher structural stability than isolated gas-phase systems. Second, higher binding energies indicated that the formation of the CAP-Gr5 model could be expected to be more favourable than the CAP-Gr3 model. Third, the values regarding electron transfers indicated that the Gr5 models could play a better role than the Gr3 models. Fourth, the maximum absorption of CAP would be shifted to longer wavelengths in the CAP-Gr models but is almost fixed for the Gr models from singular to hybrid forms. Fifth, atomic scale properties indicated that the original atomic characters could remain from the singular models to hybrid systems. Finally, the CAP-Gr models could show newer molecular properties in comparison with the singular counterparts but with fixed original atomic scale properties for the CAP counterpart; an important requirement for medicinal carriers, which should not change the properties of the carried counterpart.

References

[1] B. K. Edwards, A. M. Noone, A. B. Mariotto, E. P. Simard, F. P. Boscoe, et al., Cancer **120**, 1290 (2014).
[2] J. Nonnekens and J. H. Hoeijmakers, EMBO Mol. Med. **9**, 4 (2017).
[3] A. K. Dutta, Int. J. Appl. Eng. Res. **11**, 401 (2016).
[4] A. Ellis, M. Frey, L. Koontz, S. Shyne, J. Chern, et al., Gynecol. Oncol. **141**, 23 (2016).
[5] S. Iijima, Nature **56**, 354 (1991).
[6] A. Tay, F. E. Schweizer, and D. Di Carlo, Lab Chip **16**, 1962 (2016).
[7] W. Ding, C. Lou, J. Qiu, Z. Zhao, Q. Zhou, et al., Nanomed. Nanotechnol. Biol. Med. **12**, 235 (2016).
[8] R. P. Singh, G. Sharma, S. S. Singh, S. C. U. Patne, B. L. Pandey, et al., Mater. Sci. Eng. C **67**, 313 (2016).
[9] M. Mirzaei and R. Salamat, Superlattices Microstruct. **65**, 375 (2014).
[10] J. Liu, C. Detrembleur, S. Mornet, C. Jérôme, and E. Duguet, J. Mater. Chem. B **3**, 6117 (2015).
[11] N. Habibi, N. Kamaly, A. Memic, and H. Shafiee, Nano Today **11**, 41 (2016).
[12] X. Hao, X. Hu, C. Zhang, S. Chen, Z. Li, et al., ACS Nano **9**, 9614 (2015).
[13] A. K. Geim and K. S. Novoselov, Nat. Mater. **6**, 183 (2007).
[14] D. Seddon, Chem. Aust. 36 (2016).
[15] N. Alegret, A. Criado, and M. Prato, Curr. Med. Chem. **24**, 529 (2017).
[16] H. Sabzyan and N. Sadeghpour, Z. Naturforsch. A **72**, 1 (2017).
[17] B. Zhang, Y. Wang, J. Liu, and G. Zhai, Curr. Med. Chem. **24**, 268 (2017).
[18] M. Mirzaei, Superlattices Microstruct. **54**, 47 (2013).
[19] N. Ma, J. Liu, W. He, Z. Li, Y. Luan, et al., J. Colloid Interface Sci. **490**, 598 (2017).
[20] C. Cheng, S. Li, A. Thomas, N. A. Kotov, and R. Haag, Chem. Rev. **117**, 1826 (2017).
[21] Y. Li, Z. Jian, M. Lang, C. Zhang, and X. Huang, ACS Appl. Mater. Interfaces **8**, 17352 (2016).
[22] M. Mirzaei, M. Yousefi, and M. Mirzaei, Mod. Phys. Lett. B **25**, 1335 (2011).
[23] L. Zhou, H. Mao, C. Wu, L. Tang, Z. Wu, et al., Biosens. Bioelectron. **87**, 701 (2017).
[24] D. Rosmarin, C. Palles, D. Church, E. Domingo, A. Jones, et al., J. Clin. Oncol. **32**, 1031 (2014).
[25] S. F. Lee, C. L. Chiang, A. S. Lee, F. C. S. Wong, and S. Y. Tung, Mol. Clin. Oncol. **3**, 1398 (2015).
[26] S. P. Chandran, S. B. Natarajan, S. Chandraseharan, and M. S. B. M. Shahimi, J. Cancer Res. Pract. **4**, 45 (2017).
[27] S-B. Sun, P. Liu, F-M. Shao, and Q-L. Miao, Int. J. Clin. Exp. Med. **8**, 19670 (2015).
[28] M. Mirzaei, Int. J. Nano Dimens. **3**, 175 (2013).
[29] E. Naderi, M. Mirzaei, L. Saghaie, G. Khodarahmi, and O. Gülseren, Int. J. Nano Dimens. **8**, 124 (2017).
[30] Z. E. Hughes and T. R. Walsh, Nanoscale **7**, 6883 (2015).
[31] P. Bonnet, Eur. J. Med. Chem. **54**, 679 (2012).
[32] Q. Tang, Z. Zhou, and Z. Chen, Nanoscale **5**, 4541 (2013).
[33] Z. Qian, J. Ma, X. Shan, L. Shao, J. Zhou, et al., RSC Adv. **3**, 14571 (2013).
[34] Y. Xu, Z. Liu, X. Zhang, Y. Wang, J. Tian, et al., Adv. Mater. **21**, 1275 (2009).
[35] D. W. Boukhvalov and M. I. Katsnelson, J. Phys. Condens. Matter **21**, 344205 (2009).
[36] H. R. Masoodi, S. Bagheri, and R. Ranjbar-Karimi, Chem. Phys. Lett. **667**, 327 (2017).
[37] K. Wolinski, J. F. Hinton, and P. Pulay, J. Am. Chem. Soc. **112**, 8251 (1990).
[38] E. R. Andrew and H. Gutowsky, Am. J. Phys. **24**, 417 (1956).

[39] A. J. Cohen and N. C. Handy, Mol. Phys. **99**, 607 (2001).

[40] V. A. Rassolov, M. A. Ratner, J. A. Pople, P. C. Redfern, and L. A. Curtiss, J. Comput. Chem. **22**, 976 (2001).

[41] M. Frisch, G. Trucks, H. Schlegel, G. Scuseria, M. Robb, et al., Gaussian 09 Revision A.01, Gaussian Inc., Wallingford, CT 2009.

[42] B. Mennucci, Wiley Interdiscip. Rev. Comput. Mol. Sci. **2**, 386 (2012).

[43] A. Zeroual, A. Benharref, and A. E. Hajbi, J. Mol. Model. **21**, 44 (2015).

[44] S. M. Bouzzine, S. Bouzakraoui, M. Bouachrine, and M. Hamidi, J. Mol. Struct. **726**, 271 (2005).

[45] B. G. Johnson, P. M. W. Gill, and J. A. Pople, J. Chem. Phys. **98**, 5612 (1993).

[46] T. Quinn and P. Choudhury, Mol. Catal. **431**, 9 (2017).

[47] A. Mokhtari, K. Harismah, and M. Mirzaei, Superlattices Microstruct. **88**, 56 (2015).

[48] T. Koopmans, Physica **1**, 104 (1934).

[49] J. Frau, F. Muñoz, and D. Glossman-Mitnik, Chem. Inf. **2**, 7 (2016).

[50] J. Luo, Z. Q. Xue, W. M. Liu, J. L. Wu, and Z. Q. Yang, J. Phys. Chem. A **110**, 12005 (2006).

[51] M. Mirzaei and M. Meskinfam, Comput. Theor. Chem. **978**, 123 (2011).

[52] A. Bodaghi, M. Mirzaei, A. Seif, and M. Giahi, Physica E **41**, 209 (2008).

[53] M. Mirzaei, Monatsh. Chem. **140**, 1275 (2009).

[54] M. Mirzaei, N. L. Hadipour, and M. R. Abolhassani, Z. Naturforsch. A **62**, 56 (2007).